Temporal Analysis for the Dynamic Stability of A DC / DC Converter in a Photovoltaic System

Nacera Mazouz*, Ahmed Bengermikh, Abdelhamid Midoun
nacera.mazouz@univ-usto.dz, mazouz.usto@gmail.com
Laboratory of Power Systems and Solar Energy (L.P.S.S.E), Faculty Electrical Engineering, Department of Electronics, University of Science and Technology of Oran. U.S.T.O.M.B, PO. Box 1505 El M'naouer USTO, Oran, Algeria

Abstract – *Photovoltaic systems are subjected to a disruptive environment (variation in sunlight, temperature), which can affect the operation and performance of each element constituting the photovoltaic system, in our application we were interested in the DC / DC converter which is one of the elements constituting our system, it can also be affected by the load connected to its output, as well as the impedance output of the PV array can also affect the performance of the DC / DC converter. For this, and to avoid all these problems, the converter must be precisely modeled to better predict its dynamic behavior. Where the stability is analyzed.*
The temporal response of the converter under the VMC control revealed the magnitude of the peaks at start-up at the level of the observed quantities. We have also succeeded in introducing a tracking technique to ensure an optimal energy adaptation between the photovoltaic array (PVA) and the load, so that the PVA operates at its maximum power Point (MPP), especially for optimal use of a photovoltaic system.
Finally, the results of the temporal study obtained practically justify the results of the temporal study in simulation for the VMC mode.

Keywords*: PPM, DC / DC converter, PVA, stability, mathematical model.*

Nomenclature

R_s	PV array series resistance, Ω
R_{sh}	PV array shunt resistance, Ω
V_{PV}	PV array output voltage, V
I_{PV}	PV array output current, A
A	ideality factor (=1.92)
K	Boltzmann's constant (=1.38 · 10^{-38} K/J)
T	cell temperature, K
P_{PV}	PV array output power, W
V_O	Voltage across the load, V
I_O	Current load, A
Z_L	Load resistance, Ω
d	duty cycle ratio
i_p	current delivered by the solar cell, A
i_{ph}	current photo, created by solar photons, A
i_d	current with a diode, A
i_{sh}	shunt current, A
i_{rsh}	current flowing through the shunt resistor, A
E_{ref}	reference sunshine (=1000 w / m^2, 25 ° C).
P_1, P_2, P_3	constant parameters.
Ta	room temperature, K
N_{oct}	nominal operating temperature condition of the cell which is given by the manufacturer
I_{sat}	saturation current, A
E_g	represents the gap.
P_4	constant parameter
esr	equivalent series resistance
MPP, P	Maximum Power Point, W
C_1& C_2	Capacitors, µF
L_1& L_2	Inductors, µH
r_{L1}& r_{L2}	esr Inductors, Ω
r_{C1}& r_{C2}	esr Capacitors Ω
r_{ds}	resistance ON du MOSFET, Ω
r_d	resistance dynamic with a diode, Ω
u_{in}	input voltage, V
u_o	output voltage, V
u_{l1}	voltage across the inductor l1
u_{l2}	voltage across the inductor l2
u_{c1}	voltage across capacitor c1
u_{c2}	voltage across capacitor c2
v_{ref}	reference voltage
i_{in}	Input current, A
i_o	Output current, A
i_{L1}	current in inductance L1, A
i_{L2}	current in inductance L2, A
i_{C1}	current in capacity C1, A
i_{C2}	current in capacity C2, A
f_c	cutoff frequency, KHz
G_{ci}	command-input transfer function
G_{io}	input-output transfer function
Z_o	output impedance of the converter
G_{co}	command-output transfer function

I. Introduction

The objective of this publication is the development of a DC / DC converter for the optimization of the efficiency of a photovoltaic system, to find the most precise mathematical modeling possible allowing to predict the

behavior, and to provide information accessible to the measurement related to the physical quantities of the system, as well as the realization of an experimental prototype for the characterization of the Superbuck converter.

The search for the maximum power point is the essential work in the optimization of photovoltaic systems because there is a problem of adaptation between the load characteristics and the maximum power point of the photovoltaic generator. The optimization deals with the electrical operating parameters of the solar generator. Due to the imprecise and uncertain variation in parameters and the sensitivity to variation in intrinsic PVA parameters, modeling is strongly recommended to describe the behavior of the tracking process as shown in Fig. 1. During the last decades, several researchers have focused on the maximum power point tracking MPPT methods. The most prevalent conventional techniques, include Incremental Conductance (IC), Perturb and Observe (P&O) [2][15], Open Circuit Voltage (OCV), and Short Circuit Current (SCC) [16]. In addition to the enhancement of conventional algorithms as proposed in [12][[17][18], soft computing techniques are also a second alternative for PV power output optimization. They include mainly fuzzy logic control (FLC) [19][20][7], Artificial Neural Network (ANN) [21][22], and combined methods [23][24]. However, the determination of the reference point related to the MPP by a given algorithm in not the only problem of the PV system, since regulating and maintaining the PV output terminal to such a point is not so forward. The difficulty is due especially to the critical location of the maximum power point in a PV source characteristic, as a midpoint between two distinct behaviors. The input control design of a PV fed power stage, and the system instability is a permanent risk when the design is done assuming one input source type, since the migration of the operating point to the opposite side of the PV characteristic, changes dramatically the system dynamics. Our goal was fixed on the control of the duty cycle which will vary the voltage at its input to adapt to the maximum power. A PI regulator has been provided for this adjustment.
To have output voltage regulation, the converter must operate in closed loop; the pulse width is made proportional to the output voltage by a controller and a modulator. Fig. 5 and Fig. 12 show the converter with a feedback of the output voltage, the PID controller; its role is to reduce the error between the output voltage U_o and the reference voltage uref. The dynamics of the converter is modified by applying the feedback of the output voltage in order to analyze the stability of the latter. The results obtained by simulation have shown that the dynamics of a DC / DC converter do not only depend on its topology but also on the technology of the drive.

II. System Modeling

In this part we determine the nominal dynamic model with the VMC control technique in order to highlight its effect on the dynamics of the converter, and then we will present the simulation of mathematical models in open and closed loop to study the stability of the system.

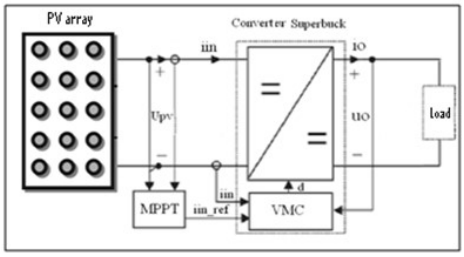

Fig. 1. The system implemented

II.1. The PV Array

The modeling of a photovoltaic module is generally used to approximate the output of the generator (voltage, current) as a function of two inputs which are the temperature and the illumination received on the plane of the module. The current generated by the photovoltaic module at a given voltage depends only on the illumination and the temperature of the cell.
The photovoltaic cell is characterized by its electrical diagram equivalent to a diode, Fig. 2, which consists of a current source and which models the conversion of the luminous flux into electrical energy, of a shunt resistor rsh which models the leakage currents in the junction (leaks through the edges of the cell and at the level of the junction), a series resistors representing the various contact and connection resistances and a diode in parallel which models the PN junction.

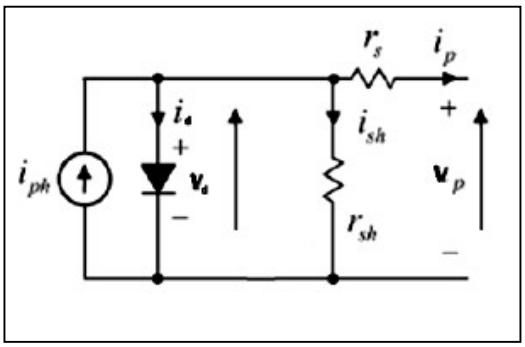

Fig. 2.Equivalent diagram of the one-diode model. [5]

$$i_p = i_{ph} - i_d - i_{sh} \qquad (1)$$

With:
i_p: The current delivered by the solar cell.
i_{ph}: Current photo, created by solar photons with energy greater than the gap.
i_d: Current of the diode.

i_{sh}: The current flowing through the shunt resistor.

The I_{ph} photocurrent depends on the amount of sunlight and the temperature of the module and can take the form of:

$$I_{ph} = P_1 * E_S * [1 + P_2 * (E_S - E_{ref}) + P_3 * (T_j - T_{ref})] \quad (2)$$

Or:

E_{ref}:the reference sunshine (1000 w / m2), the Tref is the reference temperature (25 ° C).

P_1, **P_2**, **P_3** : constant parameters.

The cell temperature can be calculated from the ambient temperature and the irradiation temperature as follows:

$$T_j = T_a + E_s.(\frac{Noct - 20}{800}) \quad (3)$$

Or:

Ta : The room temperature.

N_{oct} : The nominal operating temperature condition of the cell which is given by the manufacturer.

The bias current of the PN junction, Id, is given by the following expression:

$$I_d = I_{sat}.[\exp(\frac{q.(V_{pv} + R_s I_{pv})}{k.A.n_s.T_j}) - I] \quad (4)$$

Or:

I_{sat}:The saturation current.

k: Boltzmann constant ($1.38.10^{-23}$J/k).

q: Elementary charge (1.6×10^{-19} C).

A: Ideality factor of the junction.

The saturation current is given as follows:

$$I_{sat} = P_4.T_j^3.\exp(-\frac{E_g}{k.T_j}) \quad (5)$$

Or:

E_g: represents the gap.

P_4 : a constant parameter.

The shunt current Ish is given by the following expression:

$$I_{sh} = \frac{V_G}{R_{sh}} \quad (6)$$

We can therefore write the final equation as follows:

$$I_{pv} = P_1 \cdot E_s \cdot [1 + P_2 \cdot (E_s - E_{ref}) + P_3 \cdot (T_j - T_{ref})] - \frac{V_{pv}}{R_{sh}}$$
$$- n_p \cdot P_4 \cdot T_j^3 \cdot \exp(-\frac{E_g}{k \cdot T_j}) \cdot [\exp(\frac{q \cdot (V_{pv} + R_s \cdot I_{pv})}{k \cdot A \cdot n_s \cdot T_j}) - 1]$$

(7)

Finally, we get an implicit function of the form: **I_{pv} = f (I_{pv}, V_{pv}, Es, Tj).** With 7 parameters P_1, P_2, P_3, P_4, A, R_s and R_{sh} to be determined.

We used the parameters of the one-diode model as shown in Table (1)

TABLE 1
PARAMETERS OF THE SINGLE DIODE MODEL. [5]

The Parameters	Values
P_1	0.0035
P_2	0.00047
P_3	0.00013
P_4	86.4544
$R_{sh}(\Omega)$	105.76
$R_s(\Omega)$	0.6102
A	1

II.2. The DC/DC Superbuck Converter

Modeling by the State Space Average (SSA-M) method is one of the best for modeling DC-DC converters; it constitutes an ideal compromise between precision and simplicity.

The principle of this method is that any converter is a nonlinear system as soon as it is sequentially controlled, thus leading to a configuration with two or more linear circuits as a function of a duty cycle d (t) with two or more states. Thus, we end up with a nonlinear, variant model, controlled by a duty cycle d (t) as a function of a control signal δ (t). This model is subsequently linearized around its operating point to obtain its weak signals model which is the means of determining the various transfer functions established between its various input and output signals respectively, see Fig. 3. A Originally, this method was used only for converters operating in continuous mode (CCM) and control in voltage mode (VMC) Also called "Direct-Duty-Ratio Control, shown in Fig. 4.

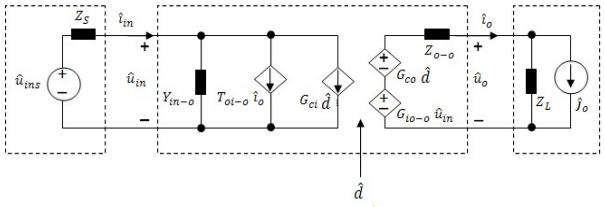

Fig. 3. Weak signal model of an open-loop DC –DC converter, supplied by a non-perfect source and delivering on a non-ideal load. [2, 4]

Thus, the different transfer functions are such as:

$$\begin{bmatrix} \hat{\imath}_{pv} \\ \hat{u}_o \end{bmatrix} = \begin{bmatrix} Y_{in-o}^{VMC} & T_{oi-o}^{VMC} & G_{ci}^{VMC} \\ G_{io-o}^{VMC} & -Z_{o-o}^{VMC} & G_{co}^{VMC} \end{bmatrix} \begin{bmatrix} \hat{u}_{pv} \\ \hat{\imath}_o \\ \hat{d} \end{bmatrix} \quad (8)$$

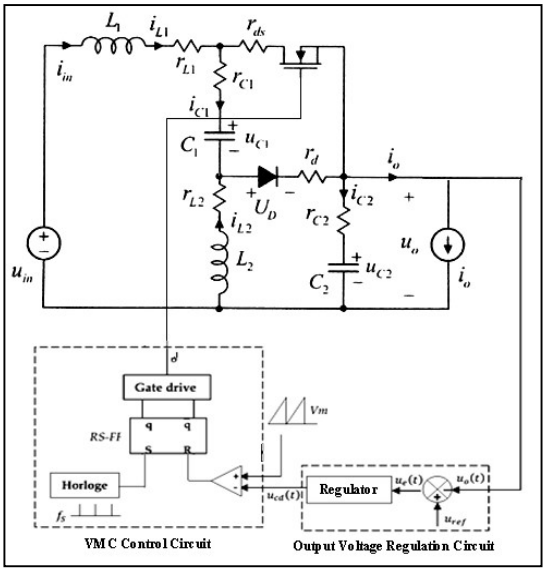

Fig. 4: Electrical diagram of the Superbuck controlled by the VMC. [6]

Where the matrix H (s) is formed by:

- H(1,1) = Y_{in-o} : the input admittance of the converter;
- H(1,2) = T_{ji-o} : the inverse transform of the output-input transfer function;
- H(1,3) = G_{ci} : command-input transfer function;
- H(2,1) = G_{io-o} : input-output transfer function;
- H(2,2) = Z_{o-o} : the output impedance of the converter;
- H(2,3) = G_{co} : command-output transfer function;
- The index "o" stands for: Open Loop.

Indeed, the transfer functions determined by equation (8) represent the internal dynamics of the converter, and they are only measurable with an ideal source ($\hat{u}_{in}$), and load ($\hat{i}_o$).

A program has been developed under Matlab and is used to determine all the transfer functions and their frequency responses for the VMC control technique.

The following study was performed on a Superbuck converter supplied with an input voltage of 20V and a desired output voltage of 10V, the circuit elements of which are summarized in Table 2 below:

TABLE 2
COMPONENT VALUES USED FOR THE STUDY OF THE SUPERBUCK CONVERTER.

The Parameters	Values	
Voltage source	Uin =20V	
Voltage across the load	Uo =10 V	
Current load	Io =2.5 A	
Inductors	L_1=15 µH	r_{L1}=80 mΩ
	L_2=15 µH	r_{L2}=55 mΩ
Capacitors	C_1=20 µF	r_{C1}=100 mΩ
Diode	U_D=0.3 V	r_d=50mΩ
load On in the MOSFET	r_{ds} =0.25Ω	
Switching frequency	f_s=440KHz	Ts=1/f_s=2.27µs
Load Resistance	R_L=4 Ω	

III. MPPT methods

The MPP technique ensures the coupling between the PV generator and the receiver by forcing the former to deliver its maximum power. One possibility would have been to set an operating point, lowering the panel voltage and at the same time increasing the current. However, this is no longer valid when the maximum power point moves. So our system (MPPT) must track the optimal operating point of the panel.

The objective of this study is to highlight the transient phenomena caused by the control on the one hand, and the disturbances at the level of the PV generator and the receiver on the other hand. The study of the stability of the system makes it possible to define the permissible range of the control and the ideal dynamic behavior.

The principle of this extreme command (MPPT) is very simple, Fig. 5 below. Starting from a command with a small duty cycle (and therefore large VPV), we increase d regularly.

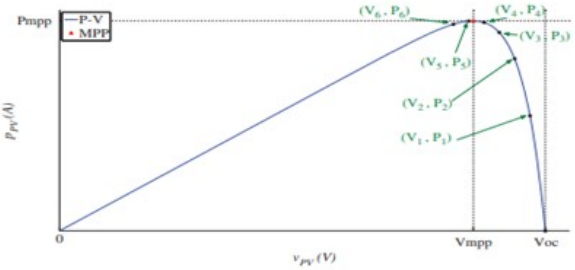

Fig. 5. Characteristic P (V) at point MPP

IV. Simulation Results

The temporal analysis of the Superbuck converter aims to observe its response as a function of time as well as the waveforms of the current and voltage, the simulation is carried out under the SIMULINK environment, the graphic extension of MATLAB which has 'a library for representing mathematical functions and systems in the form of a block diagram.

Based on the equations of states obtained, Fig. 6 illustrates the overall diagram under which the converter model is presented. The converter block must be put in the form of a quadrupole subjected to an input vector (u_{in}, i_o, d)constituting the drive signals, providing at the output the vector (i_{in}, u_o).

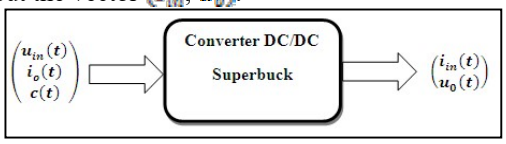

Fig. 6. Generic quadrupole form of a Superbuck DC-DC converter.

The internal structure of this quadrupole is made from the equations of the various signals existing at the circuit level as shown in Fig. 7. The block itself is made up of sub-blocks, each of which corresponds to the equation defining its output. Thus, we arrive at a model where the only parameters exchanged between its different structures are voltages and currents. This form is presented in Fig. 7 from which the observation of the waveforms of the state vectors x (t) and output u (t) provided by the corresponding outputs is possible.

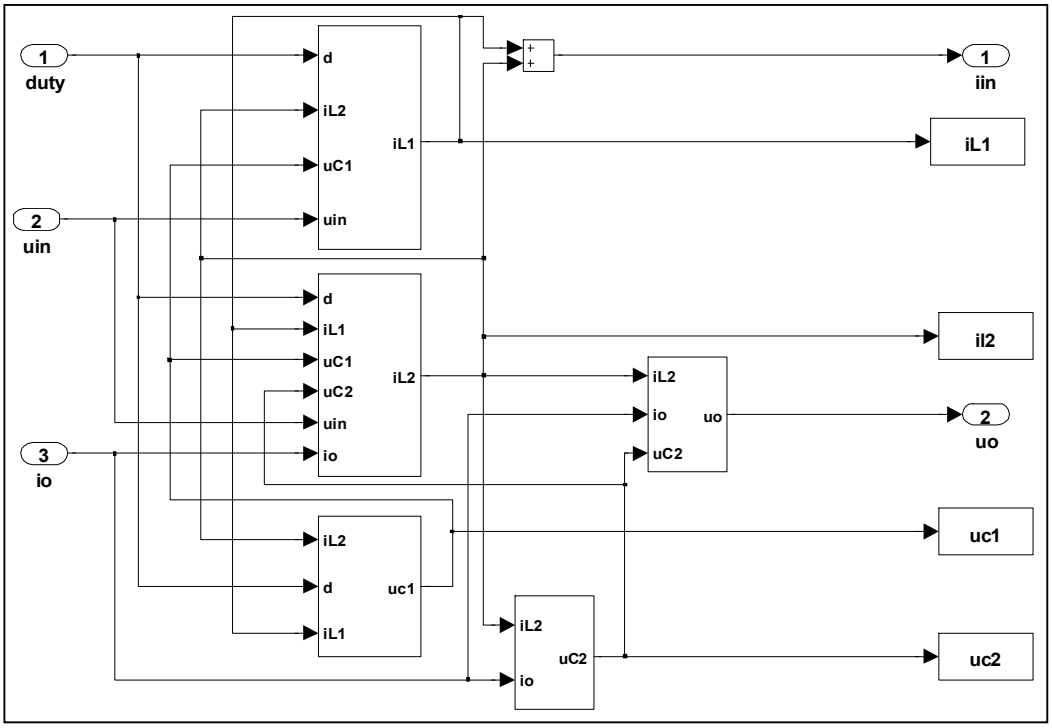

Fig. 7. Illustration of the internal structure of the Superbuck converter modeled at average values.

IV.1. Open loop control of the Superbuck controlled by VMC

The control orders of the power components are given by the strategy of the VMC, while the currents and voltages of the converter are delivered to themselves. Fig. 9 gives the block diagram of this command, from which we have determined the typical waveforms of the voltages and currents obtained at the converter.

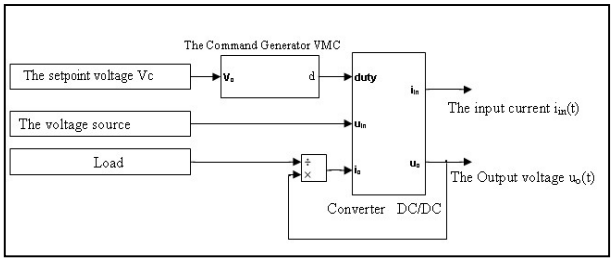

Fig. 8. Superbuck model controlled in open loop by VMC. [5]

This figure shows the converter in its quadrupole form controlled by the VMC. The input voltage is supplied by a

Perfect source of constant continuous voltage uin for the set point of the Vc control block. The load is a resistor of value R_L. The outputs can be observed at the level of the quantities: output voltage uo and the input current iin. It is also possible to observe each internal quantity of the converter thanks to the internal structure. The control commands are given by the VMC technique, it consists in comparing a set point voltage with a triangular or saw tooth carrier, the fixed frequency of which determines the switching frequency; the switch is initiated on each rising edge of the clock via an RS flip-flop; the blocking order is given when the value of the set point voltage is equal to the modulator signal. It is illustrated by Fig. 8, the generated command is presented by Fig. 9.

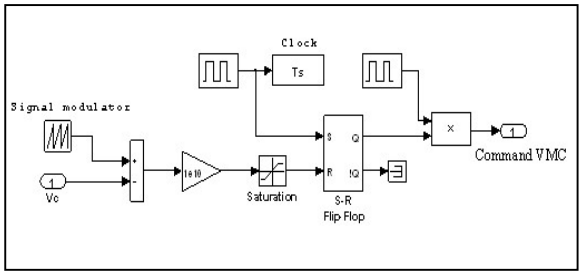

Fig. 9. Illustrative diagram of the VMC control generator. [10][11]

The waveforms of the steady-state currents in CCM mode all consist of an average value defined by the static study given in Table 1, as well as a ripple around this average value. The output current ripple is so low that it is negligible compared to its average value. The shape of these currents is shown in Fig. 10.

The same is true for the curves of the voltages $u_{C1}(t), u_{C1}(t)$ and $u_o(t)$ as shown in Fig.11.

The performance of the circuit response is evaluated from the responses of the currents and voltages, where it is observed that the input current $i_{in}(t)$ is marked by an overshoot of 15.3A evaluated at more than 4 times its average value. For the output current $i_o(t)$, an overshoot of 3.3A is observed, evaluated at more than 30% of its average value. The overshoot of the output voltage is 13.2V rated at more than 30% of its average value.

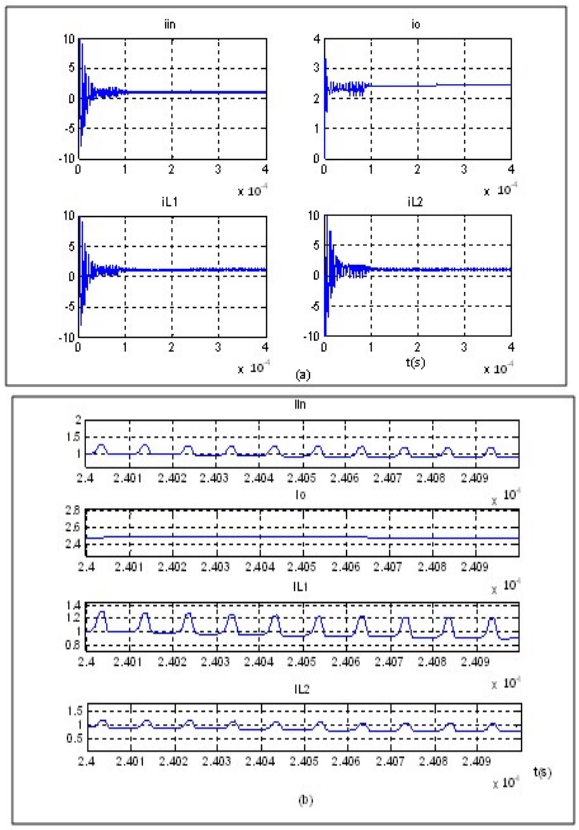

Fig. 10 : *(a)* Waveform of the currents iin (t), io (t), iL1 (t) and iL2 (t) of the Superbuck controlled in open loop by the VMC, *(b)* Waveform of steady state currents.

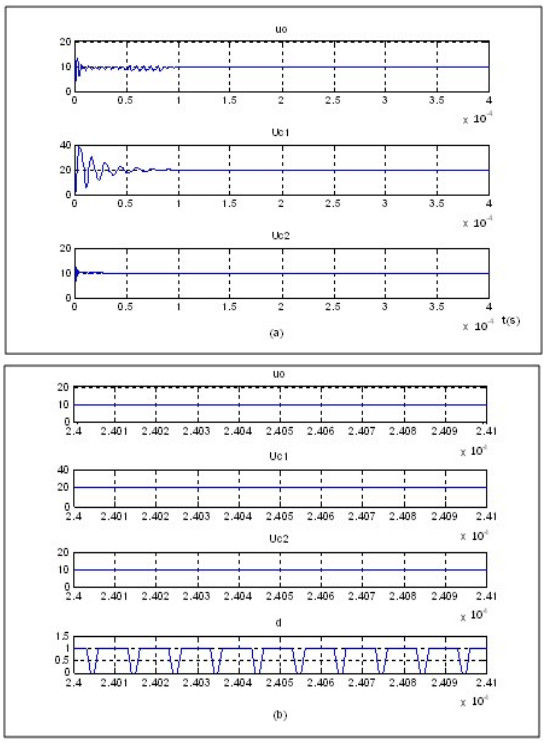

Fig. 11 : (a) Waveform of the voltages uc1 (t), uc2 (t) and uo (t) of the Superbuck controlled in open loop by the VMC , (b) Steady state voltage waveform.

IV.2. Closed loop temporal analysis

A closed loop converter is such that its control is a function of its output voltage. The block diagram of the closed loop converter is given in Fig. 12.

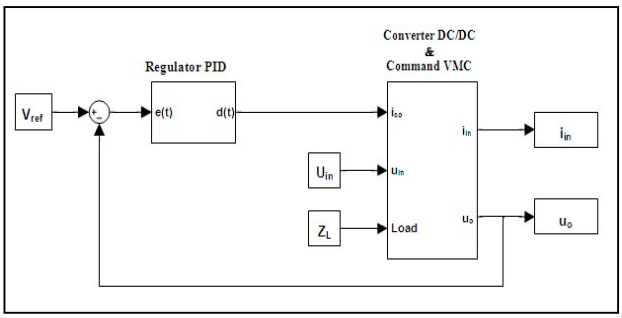

Fig. 12. Block diagram of the closed loop Superbuck converter. [5]

Establishing the feedback loop can cause a stable system to become unstable. The stability of a closed loop system can be analyzed by means of algebraic criteria among which we define the criterion of Routh, it allows to conclude to the stability, or the instability, of a controlled system from the coefficients of its characteristic polynomial whose roots make it possible to judge the stability of the system.

IV.3. Closed loop control of the Superbuck controlled by VMC

Fig. 13 shows the converter in its quadrupole form controlled by the VMC.

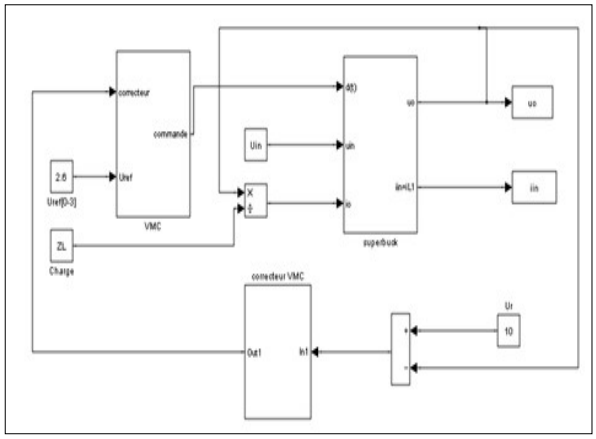

Fig. 13. Block diagram of the closed loop Superbuck converter controlled by the VMC.

The regulated output current ripple is so low that it is negligible compared to its average value. The shape of these currents is shown in Fig. 13.
The same is true for the curves of the regulated voltages $u_{c1}(t), u_{c1}(t)$ and $u_o(t)$ as shown in Fig. 14.

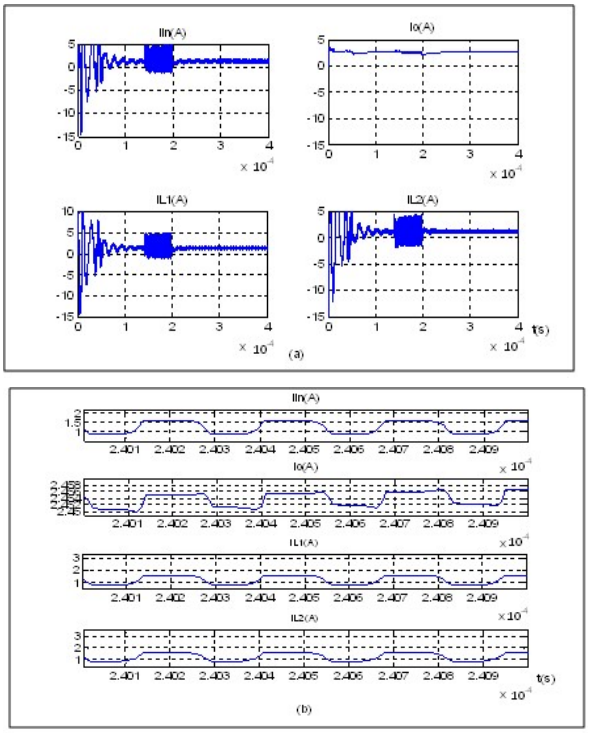

Fig. 13. (a) Waveform of the currents iL1 (t), iL2 (t), iin (t) and io (t) of the Superbuck controlled in a closed loop by the VMC; (b) Waveform of steady state currents.

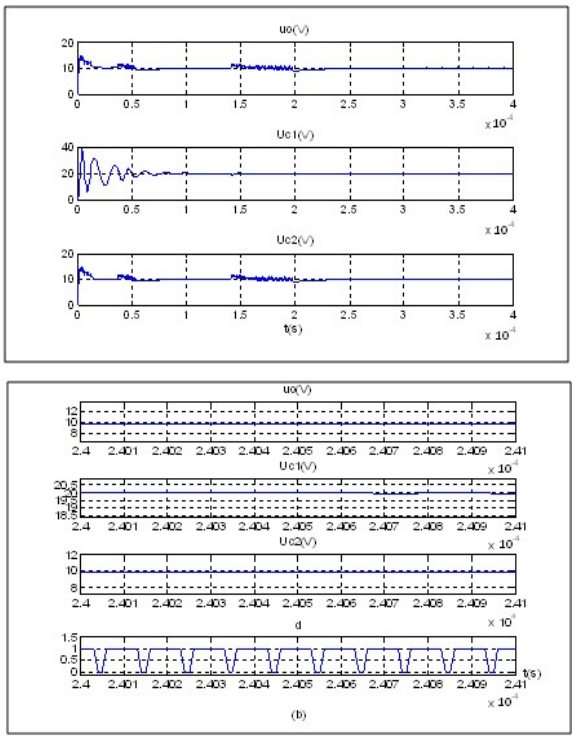

Fig. 14 . (a) Waveform of the voltages uc1 (t), uc2 (t) and uo (t) of the Superbuck controlled in a closed loop by the VMC, (b) Steady-state voltage waveform.

V. Experimental Results

This part describes the implementation of our practical work which is the realization of a prototype made up of a Superbuck converter which represents the power card and a control card based on a microcontroller of the Microchip family (Fig. 15).

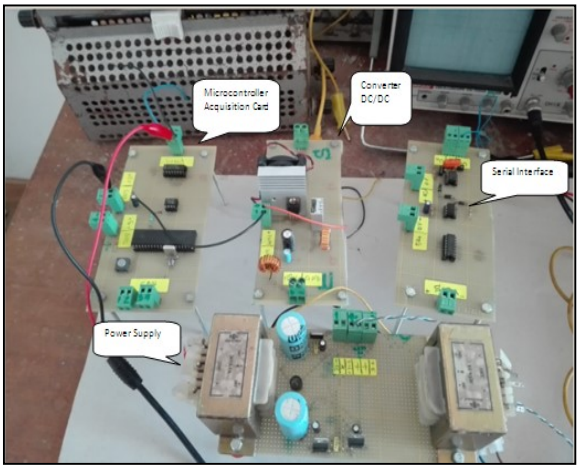

Fig.15. the System achieved;

The converter produced consists of an IRF740 Mosfet transistor, BY30F diode, two capacitors, and two inductors with the values mentioned in table 2. The MOSFET transistor is used as a switching element due to its ease of control, high efficiency, and fast switching.

Als,o the power diode which can withstand the extreme peak current of the coil is used. The regulation loohasve been implemented separatelytoo facilitate the characterization of the converter and this by usingis a microcontroller of type 18F452.

Closed Loop Converter Test

Digital control has been chosen for closeclosed-loopation, where both techniques have been implemented in the microcontroller whose output voltage control will take place (Figure 15). A PID regulator has been designed to check the stability and performance of our Superbuck converter. The 18F452 microcontroller is used to perform this task, it contains an analoanalog-to-digitalerter, a pulse generator and ,most importantly a high clock frequency. To test the performance of our regulator, two types of load (R, RLC) were used at the output of our converter.

Figure 16.a shows the time response of the converter in closa ed loop, with a variable resistive load in VMC mode. We notice that the output voltage is well regulated during the variation of the output current, on the other hand with a resonant load, we notice that the instability took place by the interconnection criterion $\frac{Z_{0\,0}}{Z_L}$, figure 16.b shows that the output voltage oscillates around the reference voltage with a frequency of 600Hz, these oscillations are caused by the disturbance generated at the level of the output current, and amplify by the interaction with the source.

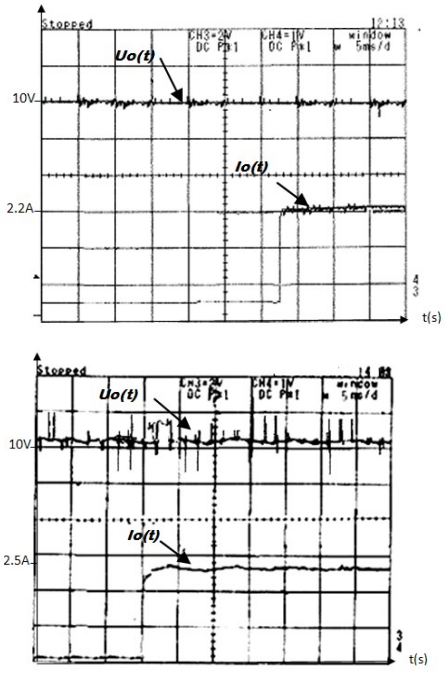

Fig.16. Time response of the converter in VMC mode. a) With resistive load. b) With resonant load.

The measurements carried out practically proved that the mathematical models give a good prediction oofthe dynamic behavior of our converter. By comparing the results of the converter's temporal responses in VMC mode (figure 16.a).

VI. Conclusion

A simulation and a realization of a prototype of the Superbuck converter were carried out itomake a comparison which allows to choose choosing which is appropriate for the given application in order to tom its advantages.

The results of the simulation allowed us to know the advantage of using a photovoltaic source. In addition, the study made for a photovoltaic source definitively proves that the operating margin of a Superbuck converter can cover the entire curve of the operating points of the PVA without observed constraints. Limiting the output voltage, however, can make the converter unstable at the maximum PPM power point.

The results of the teFrom theral responses of the converter in VMC mode for the same resistive load, we find that the response is faster, in addition to its immediate reaction to any change in voltage.

As a result, VMC reduces the effect of the resonance phenomenon that marks the harmonic responses of these controlled converters.

The intended prospects are to be able to apply both VMC and PCM (Pick Current Mode) commands on other static converters in order to benetoeir advantages and overcome problems often encountered during the analysis of power systems.

References

[1] J.Leppaho, T. Suntio, Dynamic Characteriz Sun Current-Mode-Controlled Buck Converter With Output-Current Feed super-buck Converter , IEEE TRANSACTIONS ON POWER ELECTRONICS, Vol. 26, 2011,pp.200-209.

[2] Chaicharoenaudo mrung, K., Areerak, K., Thumthae, C., Maximum Power Point Tracking Control Using P&O Method for Stand-Alone Real Wind turbine system, (2018) international review of electrical engineering (IREE), 13(1),pp.37-44.
Doi:https://doi.org /10.15866/iree.v13i1.14456

[3] M.Karppapen, M.Hankaniemi, S.Teuvo, M.Sippola, Dynamical Characterization of Input-Voltage-Feedforward-Controlled Buck Converter, *IEEE Trans. Electron. Indus*., vol. 54, no. 2, Apr. 2007.

[4] N. MAZOUZ, Implementation of A Converter DC / DC Control VMC and PCM In A Photovoltaic System, Elec. Gen. Fac., Dept. Elect. Univ. USTO, Algeria, Thesis, Jul. 02. 2014.

[6] M. Hankaniemi, M. Karppanen and T. Suntio: Dynamical Characterization of Voltage Mode Controlled Buck Converter Operating in CCM and DCM. IEEE, EPE-PEMC 2006, Portoro2, Slovenia.

[7] N. Mazouz, A. Midoun: Control of a DC/DC converter by fuzzy controller for a sothe lar pumping system. ELSEVIER, Electrical Power and Energy Systems, JEPE 1492, 27 August 2011, No. of Pages 9, Model 5G.

[8] R. D. Middlebrook: Small-Signal Modeling of Pulse-Width Modulated Switched-Mode Power Converters. Proceedings of the IEEE, Vol. 76, No. 4, April 1988.

[9] R. D. Middlebbrook & S. M. Ćuk, A General Unified Approach To Modeling Switching-Converter Power Stages. Int. Journal of Electronics, Vol. 42, No. 6, 1977, pp. 521-550.

[10] M. Karppanen, M. Hankaniemi, T. Suntio, Mika Sippola , Dynamical Characterization of Peak-Current-Mode-Controlled Buck Converter With Output-Current Feedforward , IEEE TRANSACTIONS ON POWER ELECTRONICS, Vol. 22, No. 2, March 2007.

[11] M. Karppanen, Towards Optimal Converter in Distributed Power Supply System. Master of Science Thesis. Tamper University of The Science, Department of Electrical Engineering. Tamper 27-03-2006.

[12] Mazouz N. Tracking of the optimal point of PV array through a DC/DC buck converter in a pumping solar system by fuzzy logic. Master Thesis, July 2005, Electrical Engineering Faculty, Oran, Algeria; 2005.

[13] Ding, K., Zhang, J., Xigao, Xu, B.J. A Simplified Model For Photovoltaic Modules Based O Improved Translation Equations. Solar Energy. 101, pp. 40-52 (2014).

[14] Li,Y., Huang, W., Huang, H., Witt, C.H., Chen, Y., Fag, G ad Caroll, D.L. Evaluation Of Methods To Extract Parameters From Current-Voltage Characteristics Of Solar Cells. Solar Energy. 90, pp. 51-57 (2014).

[15] N.A.Kamarsaman, C.W. Tan, A Comprehensive Review Of Maximum Power Point Tracking Algorithm For Photovoltaic Systems. Renewable And Sustainable Energy Review, vol. 37, pp. 585-598.2014.

[16] Dib, K., Chenni, R, A Combined MPPT Algorithm For Photovoltaic Systems Based Arduino Microcontroller . International Journal On Energy Conversion (IRECON). 6(2), pp.66-75,2018. Doi:https://doi.org/10.15866/irecon.v63i2.15090

[17] Hwu, K., Yau, Y., Applying Improved Boost Converter And Simple Tracking Concept To Achieving MPPT Under Shading Conditions. (2017) International Review Of Electrical Engineering (IREE), 12(3),pp.195-203.
Doi:htt ps://doi.org/10.15866/iree.v12i3.11695

[18] Fri, A., El Bachtiri, R.,Ghzizal, A., Imp roved MPPT Algorithm for Controlling a PV System Grid Connected For Rapid Changes Of Irradiance. (2016) International Review Of Automatic Control (IREACO), 9(1), pp.11-20.
Doi:https://doi.org/10.15866/ireaco.v9i1.7921

[19] Attia, H., A Stand-Alone Solar-PV System With MPPT Based On Fuzzy Logic Control For Direct Current Portable House Applications. (2018) International Review on Modeling and Simulations (IREMOS), 11(6), pp.377-385.
Doi:h ttps://doi.org/10.15866/iremos.v11i6.16074

[20] Abadi, I., Musyafa, A., Soeprijanto, A., Type-2 Fuzzy Logic Controller Based PV Passive Tow-Axis Solar Tracking System. (2015) International Review Of Electrical Engineering (IREE), 10(3), pp.390-398.
D oi :https://doi.org/10.15866/iree.v10i3.6090

[21] S.Ma, M. Chen, J. Wu. Huo, L. Huang, Augmented Nonlinear Controller For Maximum Power-Point Tracking With Artificial Neural Network In Grid-Connected Photovoltaic Systems. Energies, vol. 9 n.12, 2016,pp. 1005-102 8.

[22] Sunarno, E., Assidiq, R., Nugraha, S., Sudiharto, I., Qudsi, O., Eviningsih, R., Application Of The Artificial Neural Network (ANN) Method As MPPT Photovoltaic For DC Source Storage. (2019) International Review Of Automatic Control (IREACO), 12(3), pp.145-153.
Doi:https://doi.org/10.15866/ireaco.v12i3.16455

[23] S.Z.Hassan, H.Li, T. Kamal, U. Arifoglu, S. Mumtaz, I., Khan, Neuro-Fuzzy Wavelet Based Adative MPPT Algorithm For Photovoltaic Systems. Energies, vol. 10, 2017, pp. 394-409.

[24] Olanipekun, M., Munda, J., Hamam, Y., A Multi-Start Greedy Algorithm For Optimal Reconfiguration Of Solar Photovoltaic Arrays For Maximum Power Output In Real-Time Application. (2017) International Review Of Electrical Engineering (IREE), 12(5) ,p p.431-439.
Doi:https://doi.org/10.15866/iree.v12i5.12763